Engineering Fracture Mechanics 78 (2011) 2572–2584

Contents lists available at ScienceDirect

Engineering Fracture Mechanics

journal homepage: www.elsevier.com/locate/engfracmech

The effect of material combinations and relative crack size to the stress intensity factors at the crack tip of a bi-material bonded strip

Xin Lan *, Nao-Aki Noda, Kengo Mithinaka, Yu Zhang

Department of Mechanical Engineering, Kyushu Institute of Technology, 1-1 Sensui-cho, Tobata-ku, Kitakyushu-shi, Fukuoka 804-8550, Japan

ARTICLE INFO

Article history:
Received 11 February 2011
Received in revised form 16 June 2011
Accepted 29 June 2011

Keywords:
Stress intensity factor
Edge interface crack
Bi-material bonded plate
Material combinations
Finite element method

ABSTRACT

Several types of singular stress fields may appear at the corner where an interface between two bonded materials intersects a traction-free edge depending on the material combinations. Since the failure of the multi-layer systems often originates at the free-edge corner, the analysis of the edge interface crack is the most fundamental to simulate crack extension. In this study, the stress intensity factors for an edge interfacial crack in a bi-material bonded strip subjected to longitudinal tensile stress are evaluated for various combinations of materials using the finite element method. Then, the stress intensity factors are calculated systematically with varying the relative crack sizes from shallow to very deep cracks. Finally, the variations of stress intensity factors of a bi-material bonded strip are discussed with varying the relative crack size and material combinations. This investigation may contribute to a better understanding of the initiation and propagation of the interfacial cracks.

1. Introduction

Most failure for the bonded structures initiates at the interfacial edge corner due to the existence of free edge singularities under mechanical or thermal loadings. A lot of pioneering studies were addressed on the stress singularities around bi-material corners and joints. As an example, the geometrical configuration as shown in Fig. 1 is characterized by the angles θ_1 and θ_2 which the traction-free surfaces of the elastic materials make with the interface. Several types of stress singularities appear at the interface corner depending on the geometry and material combinations for this bonded layer. Many papers discussed the order of the stress singularity under various geometries and material combinations [1–6]. Also a fair mount of attentions were paid for the intensity of this singular stress. Reedy and Guess [7] determined the magnitude of singular stress for a thin elastic layer sandwiched between two rigid substrates. Akisanya and Fleck [8] applied the contour integral to evaluate the singular stress at the free-edge of a long bi-material strip subjected to uniform tension. Xu et al. [9] proposed numerical methods to determine the multiple stress singularities and the related stress intensity coefficients.

On the other hand, the evaluation of the stress intensity factors for the interfacial cracks has some difficulties due to the complexity of multiple/oscillatory singularities. Various numerical methods [10–14] were reported to determine the stress intensity factors of an interface crack. Specifically, Teranishi and Nisitani proposed a highly accurate numerical method named the zero element method to determine the stress intensity factor of a homogenous plate [15]. Anyway, this method cannot be used directly into the interface crack problem since there is an oscillatory singularity along the interface. Then, Oda et al. extended this method to the interface crack problems by creating the similar singular stress fields for the reference and the given unknown problems [14]. None of the aforementioned studies has considered the stress intensity factors for arbitrary combination of materials and relative crack size. Noda et al. investigated the stress intensity factors for arbitrary

* Corresponding author.
E-mail address: xinlan_al@yahoo.com (X. Lan).

0013-7944/$ - see front matter © 2011 Elsevier Ltd. All rights reserved.
doi:10.1016/j.engfracmech.2011.06.017

Nomenclature

a	length of the edge interface crack
$f_{ij}(\theta)$	angular functions
r	polar distance away from the singular point/crack tip
E_m	Young's modulus
F_1, F_2	dimensionless stress intensity factors at the crack tip of an edge interface crack
G_m	shear modulus
H	intensity of stress singularity
L	height of the bonded strip
K	stress intensity factors
K_1, K_2	general stress intensity factors at the crack tip of an edge interface crack
W	width of the bonded strip
T, S	tensile and shear stresses applied to the reference problem
α, β	material composite parameters
θ_1, θ_2	angles of traction-free edges intersect the interface
κ	Kolosov constant
λ	order of the stress singularity
σ_y, τ_{xy}	stress components along the bi-material interface
$\sigma^*_{y0,FEM}, \tau^*_{xy0,FEM}$	stress components at the crack tip of the reference problem
$\sigma_{y0,FEM}, \tau_{xy0,FEM}$	stress components at the crack tip of the given unknown problem
ν_m	Poisson's ratio

material combinations of the central interface crack in a dissimilar bonded plane [16,17]. As a further research of the author's previous work, the study object is extended to the single edge interface crack of a bonded strip. In this paper, therefore, the stress intensity factors will be investigated in a bi-material bonded finite strip as shown in Fig. 2 by applying the finite element method with varying not only the material combinations but also the relative crack sizes. The material combinations (α, β) vary $\alpha = 0$–0.95, $\beta = -0.2$ to 0.45 in the α–β space, and the relative crack size a/W varies from the shallow crack to the very deep crack. Furthermore, we will show that the stress intensity factors behave a good linearity to the crack length within the zone of dominance of the free edge singularity. Then, a formula will be proposed to determine the stress intensity factors for the shallow edge interface cracks under arbitrary combination of materials and relative crack size, by fitting the computed results.

2. Numerical method for the determination of the stress intensity factors

Recently, an effective numerical method called the zero element method was proposed for calculating the stress intensity factors in homogenous cracked plates [15]. Then, the method is successfully extended to the interfacial crack problems [14,16,17]. Both of those methods utilize the stress values at the crack tip computed by FEM. For a given bi-material bonded structure, the stress intensity factors are defined as shown in:

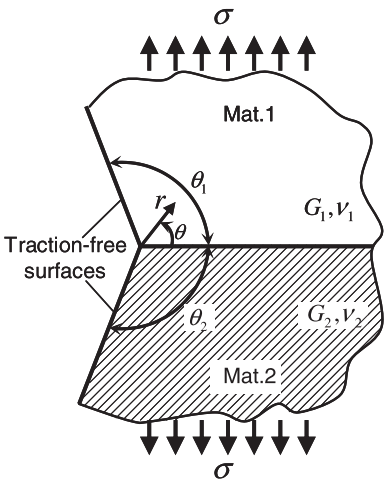

Fig. 1. Geometrical configuration of bi-material bonded plate.

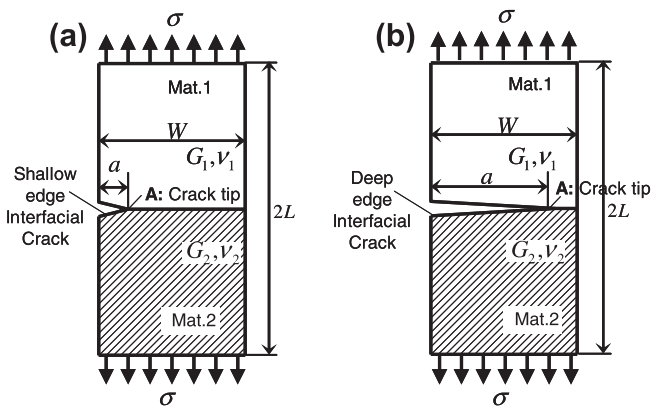

Fig. 2. The shallow (a) and deep (b) edge interface cracks in a bonded strip.

$$\sigma_y + i\tau_{xy} \to \frac{K_1 + iK_2}{\sqrt{2\pi r}} \left(\frac{r}{2a}\right)^{i\varepsilon}, \quad r \to 0 \tag{1}$$

Here, σ_y, τ_{xy} denote the stress components near the crack tip. r is the radial distance from the crack tip, and ε is the bi-elastic constant given by:

$$\varepsilon = \frac{1}{2\pi} \ln\left[\left(\frac{\kappa_1}{G_1} + \frac{1}{G_2}\right) \Big/ \left(\frac{\kappa_2}{G_2} + \frac{1}{G_1}\right)\right] \tag{2}$$

$$\kappa_m = \begin{cases} 3 - 4\nu_m \text{ (plane strain)} \\ 3 - \nu_m / 1 + \nu_m \text{ (plane stress)} \end{cases}, \quad (m = 1, 2) \tag{3}$$

where $G_m (m = 1, 2)$ and $\nu_m (m = 1, 2)$ are the shear moduli and Poisson's ratios of either respective materials. The real and imaginary parts of the oscillatory stress intensity factors $K_1 + iK_2$ in Eq. (1) may be separated as

$$K_1 = \lim_{r \to 0} \sqrt{2\pi r}\sigma_y \left(\cos Q + \frac{\tau_{xy}}{\sigma_y} \sin Q\right) \tag{4}$$

$$K_2 = \lim_{r \to 0} \sqrt{2\pi r}\tau_{xy} \left(\cos Q - \frac{\sigma_y}{\tau_{xy}} \sin Q\right) \tag{5}$$

$$Q = \varepsilon \ln\left(\frac{r}{2a}\right) \tag{6}$$

Let's consider two different interface crack problems C and D. The geometric configurations for problems C and D are demonstrated in Fig. 3a and b, respectively. The stress intensity factors of problem C are given in advance and those for

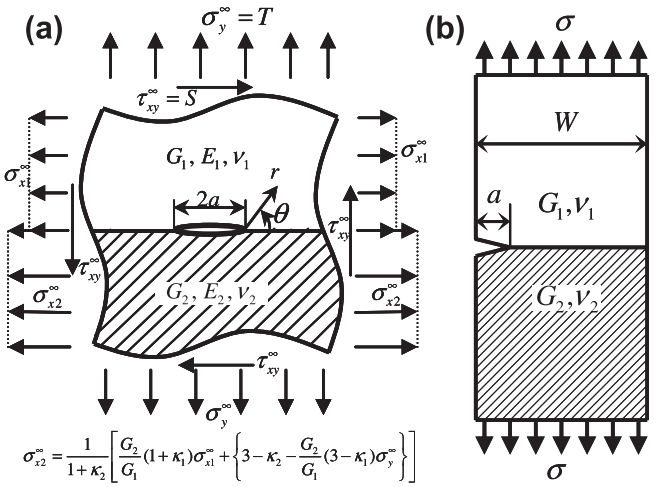

Fig. 3. Demonstration of: (a) the reference problem (problem C) and (b) a given unknown problem (problem D).

problem D are yet to be solved. For notional convenience, problem C is termed the reference problem whose values are marked with *, and problem D is termed the given unknown problem. Assuming they have the same crack lengths (half length) $a = a_0$ and the same combination of materials $\varepsilon = \varepsilon_0$. Examining the points with the same radial distances $r = r_0$ for the two problems C and D, then gives $[Q^*]_C = [Q]_D = \varepsilon_0 \ln(\frac{r_0}{2a_0})$. Recall Eqs. (4) and (5), a proportional relationship given in Eq. (7) is established if and only if Eq. (8) can be satisfied,

$$\frac{[K_1]_D}{[K_1^*]_C} = \frac{[\sigma_y]_D}{[\sigma_y^*]_C} = \frac{[\sigma_{y0.FEM}]_D}{[\sigma_{y0.FEM}^*]_C}, \frac{[K_2]_D}{[K_2^*]_C} = \frac{[\tau_{xy}]_D}{[\tau_{xy}^*]_C} = \frac{[\tau_{xy0.FEM}]_D}{[\tau_{xy0.FEM}^*]_C} \tag{7}$$

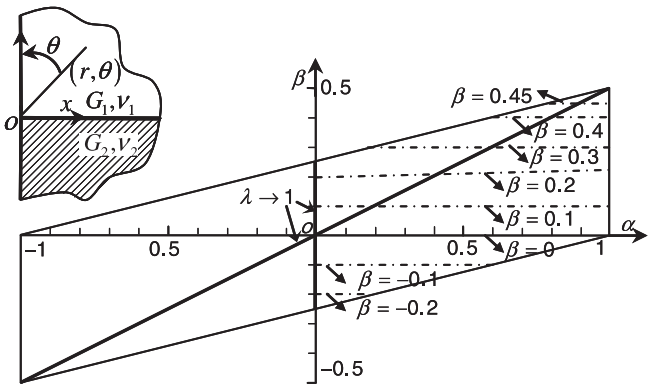

Fig. 4. α–β space for the material composite parameters.

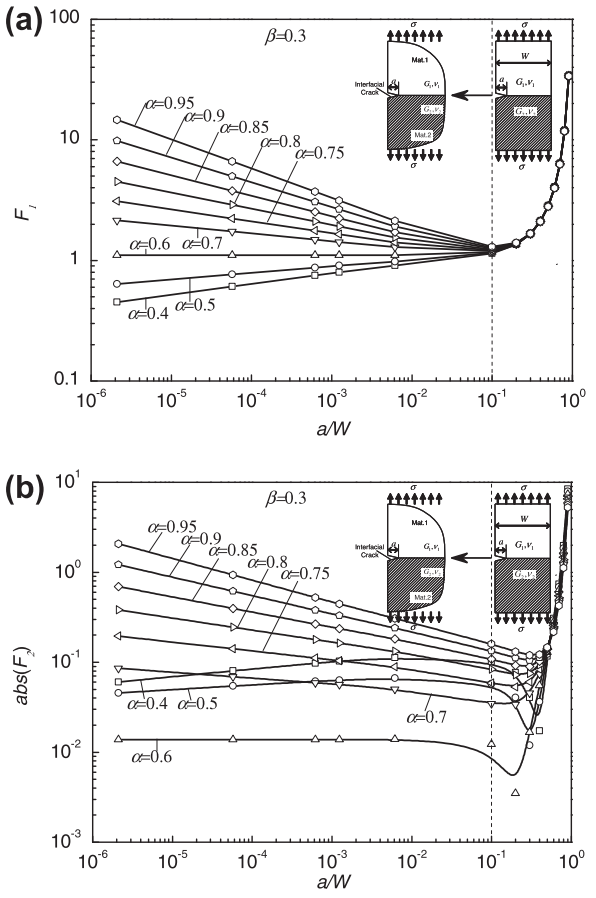

Fig. 5. The double logarithmic distributions of the dimensionless stress intensity factors: (a) F_1 and (b) F_2 at the crack tip for shallow edge interface cracks.

$$\left[\frac{\tau^*_{xy}}{\sigma^*_y}\right]_C = \left[\frac{\tau_{xy}}{\sigma_y}\right]_D, \left[\frac{\tau^*_{xy0,FEM}}{\sigma^*_{y0,FEM}}\right]_C = \left[\frac{\tau_{xy0,FEM}}{\sigma_{y0,FEM}}\right]_D \tag{8}$$

Rearranging Eq. (7), then the stress intensity factors of the target given unknown problem (problem D) can be obtained by:

$$[K_1]_D = \frac{[\sigma_{y0,FEM}]_D[K^*_1]_C}{[\sigma^*_{y0,FEM}]_C}, \quad [K_2]_D = \frac{[\tau_{xy0,FEM}]_D[K^*_2]_C}{[\tau^*_{xy0,FEM}]_C} \tag{9}$$

Here, $\sigma^*_{y0,FEM}, \tau^*_{xy0,FEM}$ are the stress components at the crack tip (the zero element) of the reference problem (problem C) computed by FEM, and $\sigma_{y0,FEM}, \tau_{xy0,FEM}$ are those of the given unknown problem (problem D). The superscript 0 stands for the values at the crack tip. In this study, a central cracked bonded dissimilar plane subjected to remote uniform tension $\sigma^\infty_y = T$ and $\tau^\infty_{xy} = S$ as shown in Fig. 3a is treated as the reference problem. And its stress intensity factors are given by the theoretical solution as

$$K^*_1 + iK^*_2 = \left(\sigma^\infty_y + i\tau^\infty_{xy}\right)\sqrt{\pi a}(1 + 2i\varepsilon), \quad \sigma^\infty_y = T, \tau^\infty_{xy} = S \tag{10}$$

How to make the condition given in Eq. (8) be satisfied will be depicted in the following. Let $\sigma^{T=1,S=0*}_{y0,FEM}$ and $\tau^{T=1,S=0*}_{xy0,FEM}$ denote the stress components for the reference problem (problem C) subjected to pure remote tension $(T, S) = (1, 0)$, and $\sigma^{T=0,S=1*}_{y0,FEM}\tau^{T=0,S=1*}_{xy0,FEM}$ denote those for problem C subjected to pure remote shear $(T, S) = (0, 1)$.Using the principle of superposition, the stress components of the reference problem shown in Fig. 3a take the following form:

$$\sigma^*_{y0,FEM} = \sigma^{T=1,S=0*}_{y0,FEM} \times T + \sigma^{T=0,S=1*}_{y0,FEM} \times S \tag{11}$$

$$\tau^*_{xy0,FEM} = \tau^{T=1,S=0*}_{xy0,FEM} \times T + \tau^{T=0,S=1*}_{xy0,FEM} \times S \tag{12}$$

Recall the necessary condition given in Eq. (8) for creating the similar singular fields for the problems C and D, inserting Eqs. (11), (12) into Eq. (8) gives the solution of S/T for determining the remote external loads applied to the reference problem.

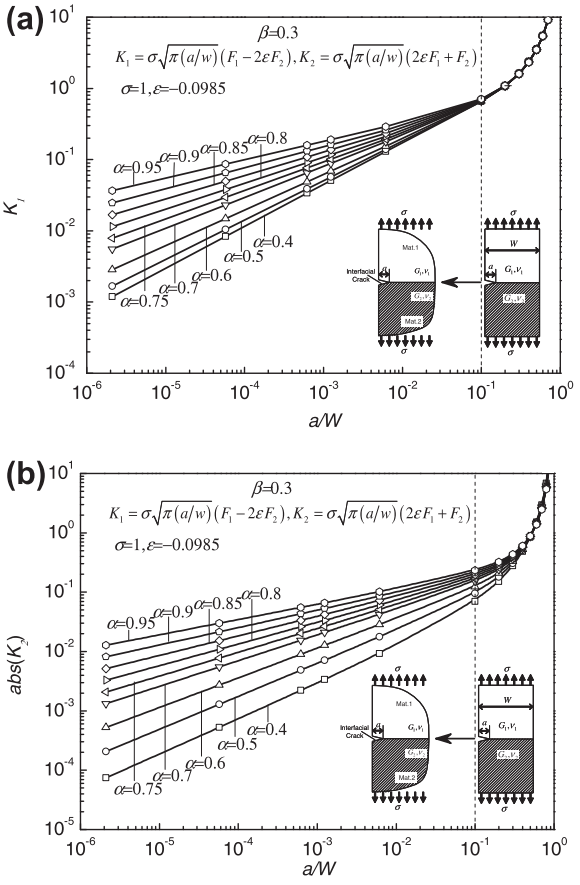

Fig. 6. The double logarithmic distributions of the stress intensity factors K_1 and K_2 at the crack tip for shallow edge interface cracks.

$$\frac{S}{T}=\frac{[\sigma_{y0,FEM}]_D\times\left[\tau_{xy0,FEM}^{T=1,S=0*}\right]_C-[\tau_{xy0,FEM}]_D\times\left[\sigma_{y0,FEM}^{T=1,S=0*}\right]_C}{[\tau_{xy0,FEM}]_D\times\left[\sigma_{y0,FEM}^{T=0,S=1*}\right]_C-[\sigma_{y0,FEM}]_D\times\left[\tau_{xy0,FEM}^{T=0,S=1*}\right]_C} \tag{13}$$

Let $T = 1$ so that S can be determined. Inserting $T = 1, S$ into Eq. (10) gives the values of the oscillatory stress intensity factors for the reference problem (problem C). Finally, the stress intensity factors for the given unknown problem (problem D) can be yielded using the proportional relationship as given in Eq. (9).

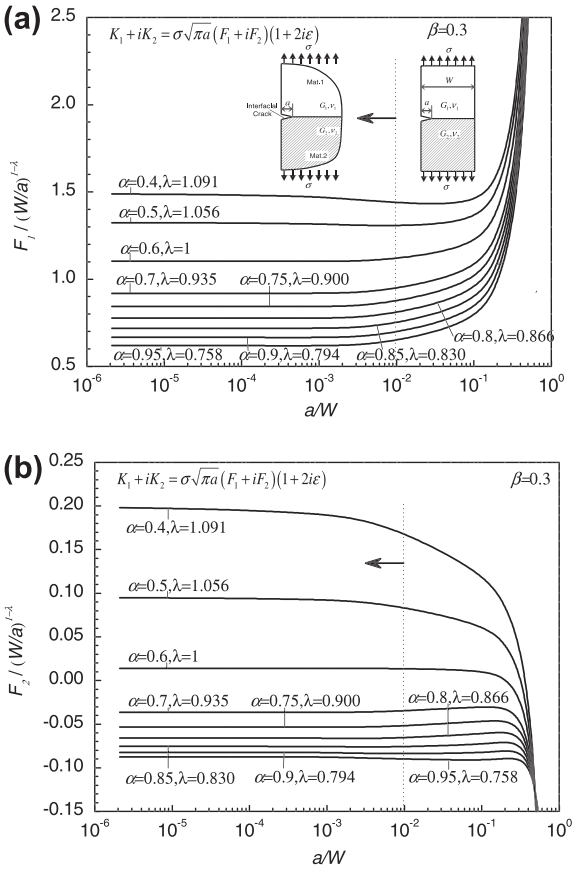

Fig. 7. The values of: (a) $F_1 \cdot (a/W)^{1-\lambda}$ and (b) $F_2 \cdot (a/W)^{1-\lambda}$ for $\beta = 0.3$.

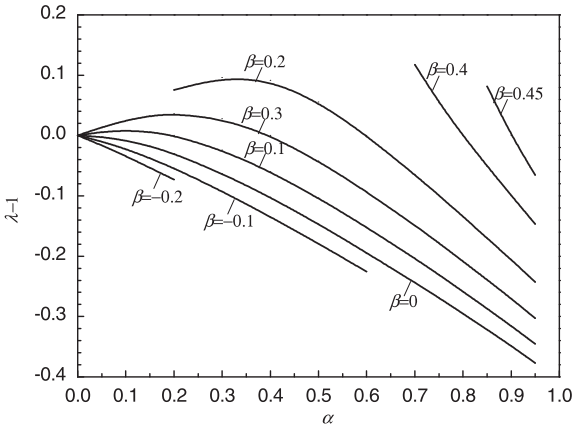

Fig. 8. Order of stress singularity $\lambda - 1$.

3. Numerical results and discussion

3.1. Formulation of the interface crack problems for arbitrary material combinations

Consider the bi-material bonded strip with width W and length $2L$ as is shown in Fig. 2. The strip is composed of two elastic, isotropic and homogeneous finite strips that are perfectly bonded along the interface. The material above the interface is termed material 1, and the material below is termed material 2. The half length of the strip L is assumed to be much greater than the width W ($L \geqslant 2W$). It is supposed that an edge interface crack with a length of a has initiated at the free-edge corner, and the strip is subjected to an axial longitudinal uniform tensile stress σ.

Table 1
Order of stress singularity λ for various combination of materials.

α	$\beta = -0.2$	$\beta = -0.1$	$\beta = 0$	$\beta = 0.1$	$\beta = 0.2$	$\beta = 0.3$	$\beta = 0.4$	$\beta = 0.45$
0	1	1	1	1	1			
0.05	0.98378	0.99035	0.99800	1.00613	1.01403			
0.1	0.96593	0.97774	0.99205	1.00831	1.02512			
0.15	0.94684	0.96269	0.98253	1.00626	1.03279			
0.2	0.92685	0.94571	0.96987	1	1.03604	1.07562		
0.3		0.90752	0.93713	0.97605	1.02764	1.09640		
0.4		0.86549	0.89741	0.94025	1	1.09130		
0.5		0.82096	0.85320	0.89662	0.95796	1.05584		
0.6		0.77459	0.80597	0.84801	0.90711	1		
0.7			0.75644	0.79606	0.85104	0.93477	1.11741	
0.75			0.73090	0.76909	0.82169	0.90048	1.05468	
0.8			0.70481	0.74151	0.79163	0.86554	1	
0.85			0.67824	0.71331	0.76091	0.83006	0.94923	1.08125
0.9			0.65105	0.68448	0.72953	0.79410	0.90075	1
0.95			0.62320	0.65496	0.69745	0.75761	0.85364	0.93488
1			0.59461	0.62466	0.66461	0.72053	0.80731	0.87624

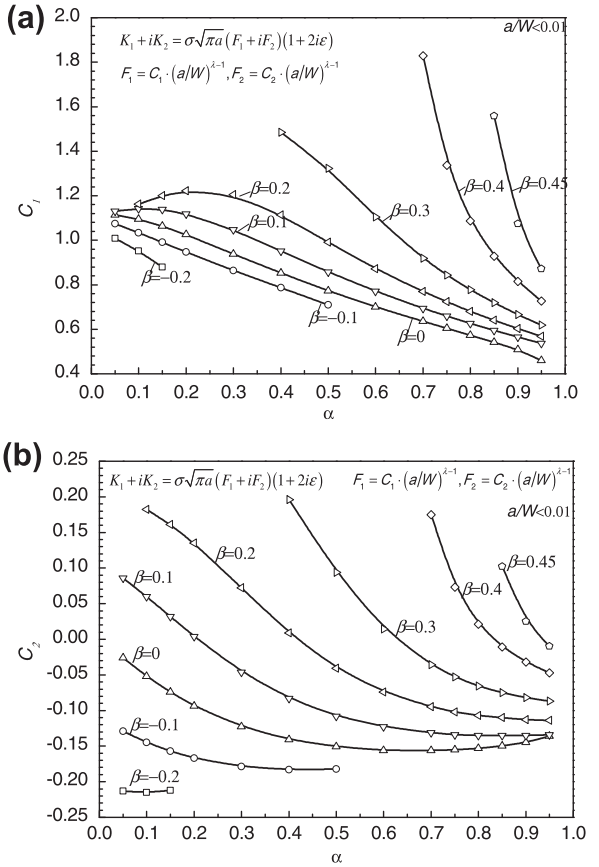

Fig. 9. Constants: (a) C_1 and (b) C_2 for various combination of materials.

The stress intensity factors for the aforementioned problem in plane strain or plane stress are only determined on the two elastic mismatch parameters α and β (also known as *Dundurs' material composite parameters*, Dundurs, 1969). And the material composite parameters are defined as

$$\alpha = \frac{G_1(\kappa_2+1) - G_2(\kappa_1+1)}{G_1(\kappa_2+1) + G_2(\kappa_1+1)} \tag{14}$$

$$\beta = \frac{G_1(\kappa_2-1) - G_2(\kappa_1-1)}{G_1(\kappa_2+1) + G_2(\kappa_1+1)} \tag{15}$$

where the subscripts denote material 1 or 2, $G_m = E_m/2(1+\nu_m)$, $(m = 1, 2)$, G_m, E_m ν_m and κ_m denote the shear modulus, Young's modulus, Poisson's ratio and Kolosov constant for material m, respectively. $\kappa_m = (3-\nu_m)/(1+\nu_m)$ for plane stress and $\kappa_m = (3-4\nu_m)$ for plane strain. The parameter α is positive when material 2 is more compliant than material 1, and is negative when material 2 is stiffer than material 1 [8]. The possible values for α and β are plotted in the α–β space shown in Fig. 4. In this research, only the stress intensity factors for $\alpha \geqslant 0$ in α–β space has been calculated due to the point symmetry of the stress intensity factors for arbitrary (α, β). For instance, switching material 1 and 2 ($mat1 \Longleftrightarrow mat2$) will only reverse the signs of α and β ($(\alpha,\beta) \Longleftrightarrow (-\alpha,-\beta)$). Furthermore, when $\alpha = \pm 1$, ν_m should be set to 0.5 or 0, follows with the pointless of analysis, therefore, 0.95 is chosen as the maximum value of α used in the analysis. The dimensionless stress intensity factors F_1 and F_2 are employed in this research, and the relationship of F_1, F_2 and K_1, K_2 is given by the following equation.

$$K_1 + iK_2 = \sigma\sqrt{\pi a}(F_1 + iF_2)(1 + 2i\varepsilon) \tag{16}$$

3.2. Relationship between the stress intensity factors and crack length

The dimensionless stress intensity factors F_1 and F_2 at the crack tip in a bi-material bonded strip are systematically investigated with varying the relative crack length *a*/*W*, as well as the material composite parameters α and β. Here, we restrict

Table 2
Tabulated values of C_1.

α	$\beta = -0.2$	$\beta = -0.1$	$\beta = 0$	$\beta = 0.1$	$\beta = 0.2$	$\beta = 0.3$	$\beta = 0.4$	$\beta = 0.45$
0.05	1.009	1.074	1.114	1.131				
0.1	0.952	1.034	1.094	1.142	1.163			
0.15	0.88	0.991	1.063	1.138	1.2			
0.2		0.947	1.025	1.119	1.222			
0.3		0.863	0.938	1.047	1.205			
0.4		0.786	0.852	0.952	1.114	1.485		
0.5		0.71	0.772	0.857	0.991	1.322		
0.6			0.7	0.771	0.872	1.104		
0.7			0.635	0.694	0.769	0.919	1.828	
0.75			0.604	0.659	0.723	0.843	1.336	
0.8			0.573	0.626	0.68	0.777	1.087	
0.85			0.542	0.595	0.64	0.719	0.928	1.558
0.9			0.508	0.565	0.603	0.666	0.815	1.075
0.95			0.46	0.536	0.568	0.619	0.727	0.871

Table 3
Tabulated values of C_2.

α	$\beta = -0.2$	$\beta = -0.1$	$\beta = 0$	$\beta = 0.1$	$\beta = 0.2$	$\beta = 0.3$	$\beta = 0.4$	$\beta = 0.45$
0.05	−0.213	−0.129	−0.026	0.086				
0.1	−0.215	−0.145	−0.052	0.06	0.182			
0.15	−0.212	−0.157	−0.074	0.032	0.161			
0.2		−0.167	−0.094	0.004	0.135			
0.3		−0.179	−0.123	−0.046	0.072			
0.4		−0.183	−0.141	−0.083	0.009	0.196		
0.5		−0.182	−0.151	−0.108	−0.041	0.094		
0.6			−0.156	−0.123	−0.074	0.014		
0.7			−0.156	−0.131	−0.095	−0.036	0.175	
0.75			−0.155	−0.134	−0.102	−0.053	0.073	
0.8			−0.153	−0.135	−0.107	−0.066	0.021	
0.85			−0.15	−0.135	−0.11	−0.075	−0.011	0.102
0.9			−0.145	−0.135	−0.113	−0.082	−0.032	0.025
0.95			−0.136	−0.134	−0.114	−0.087	−0.047	−0.010

our discussion to material combinations with $\beta = 0.3$, but similar phenomenon can also be found in others material combinations. The double logarithmic distributions of F_1 and $|F_2|$ are shown in Fig. 5a and b, respectively. It should be noted that the absolute values $|F_2|$ are used since the domain of the logarithmic function is given by the interval of $(0, +\infty)$. However, this does not affect the analysis due to the fact that switching material 1 and 2 ($mat1 \Longleftrightarrow mat2$) will only reverse the sign of F_2. From this figure, it is found that the double logarithmic distributions behave linearity when $a/W < 0.01$. Furthermore, it has been found that the slope coincides with the corresponding value of the order of singularity λ for the bonded strip [18]. In other words, the values F_1 and F_2 behave good linearity within the zone of dominance of the free-edge singularity. Fig. 5 also reveals that the sign of the slope varies depending on the sign of $\alpha(\alpha - 2\beta)$. Specifically, the slope of each line is positive when $\alpha(\alpha - 2\beta) < 0$, is zero when $\alpha(\alpha - 2\beta) = 0$ and is negative when $\alpha(\alpha - 2\beta) > 0$. Thus, it can also be deduced that the values of F_1 and F_2 for the limiting case $a/W \to 0$, are $F_1 \to 0$ and $F_2 \to 0$ when $\alpha(\alpha - 2\beta) < 0$, $F_1 \to \infty$ and $F_2 \to \infty$ when $\alpha(\alpha - 2\beta) > 0$, and F_1, F_2 have finite values when $\alpha(\alpha - 2\beta) = 0$.

Although when $\alpha(\alpha - 2\beta) > 0$ $F_1 \to \infty$ and $F_2 \to \infty$ as $a/W \to 0$, actual crack extension along the interface may be controlled by the stress intensity factors K_1, K_2 instead of dimensionless factors F_1, F_2. In order to simulate the crack extension it is important to consider how the values of K_1, K_2 change depending on the crack length. The relative crack length a/W is substituted into Eq. (16) in order to compare K_1, K_2 with F_1, F_2. The double logarithmic distributions of the stress intensity factors K_1 and K_2 are plotted in Fig. 6. A good linear relationship within the dominance of the free-edge singularity can also be found from this figure. Then, it can be deduced that $K_1 \to 0$, $K_2 \to 0$ as $a \to 0$ for any combination of materials. Here, it should be noted that the stress intensity factors always increase with increasing the crack length for all the material combinations.

3.3. Asymptotic expressions for a shallow edge interface crack in the bonded strip

The values of $F_1 \cdot (a/W)^{1-\lambda}$ and $F_2 \cdot (a/W)^{1-\lambda}$ are plotted against logarithmic relative crack size a/W in Fig. 7a and b, respectively. Here, λ denotes the singular index for a perfectly bonded strip without crack. The material composite parameters are kept in $\beta = 0.3$, but similar phenomenon can be found from other material combinations. As can be seen from these figures, the value for a given material combination approaches to a constant when $a/W < 0.01$. This is because the limiting

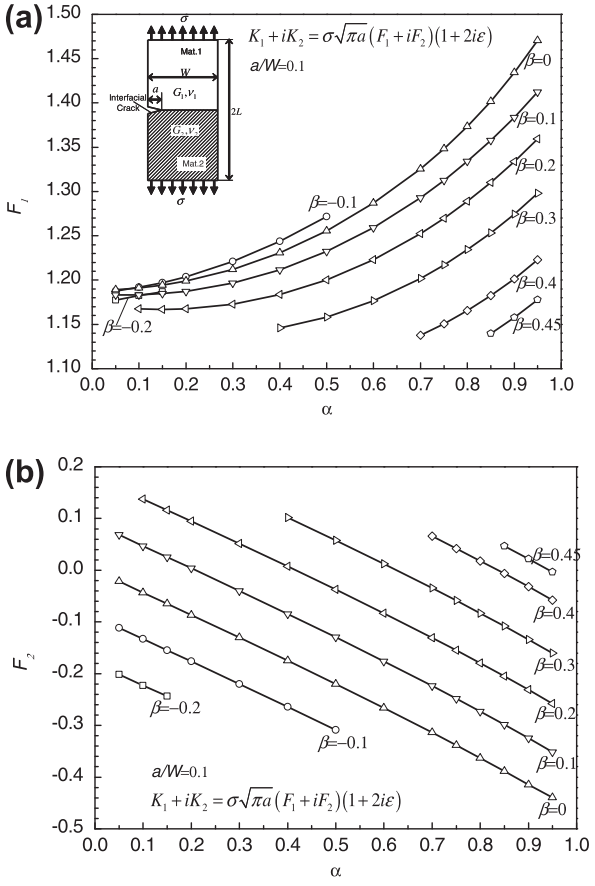

Fig. 10. Variations of: (a) F_1 and (b) F_2 with α, β for $a/W = 0.1$.

solutions $a/W \to 0$ are controlled by the singular behavior of perfectly bonded strip [18]. Thus, we propose the following formula to compute the stress intensity factors at the crack tip for the shallow edge interface crack in a bonded strip.

$$F_1 \cdot (a/W)^{1-\lambda} = C_1, F_2 \cdot (a/W)^{1-\lambda} = C_2 \tag{17}$$

In Eq. (17), the singular index λ has been investigated for various corner geometries and material combinations [2,3]. The values of λ for the current problem can be obtained by solving the following equation [2,19,20]:

$$\left[\cos^2\left(\frac{\pi}{2}\lambda\right) - (1-\lambda)^2\right]^2 \beta^2 + 2(1-\lambda)^2\left[\cos^2\left(\frac{\pi}{2}\lambda\right) - (1-\lambda)^2\right]\alpha\beta + (1-\lambda)^2[(1-\lambda)^2 - 1]\alpha^2 + \cos^2\left(\frac{\lambda\pi}{2}\right)\sin^2\left(\frac{\lambda\pi}{2}\right) = 0 \tag{18}$$

In this research, the values of λ are systematically computed for $\alpha = 0$–0.95, $\beta = -0.2$ to 0.45, the results are plotted and tabulated in Fig. 8 and in Table 1, respectively. Here, it should be noticed that λ for $\alpha < 0$ can also be obtained from Table 1 since $\lambda(\alpha, \beta) = \lambda(-\alpha, -\beta)$. The values of C_1, C_2 in Eq. (17) are constants depending upon the relative elastic properties of materials. The coefficients C_1, C_2 are plotted and listed against material composite parameters in Fig. 9a and Table 2 as well as in Fig. 9b and Table 3, respectively.

3.4. Effect of material composite parameters α, β on F_1, F_2

In this section, the effect of the material composite parameters α, β to F_1, F_2 is investigated for fixed relative crack length a/W. Figs. 10 and 11 show the variations of F_1, F_2 for $a/W = 0.1$ and $a/W = 0.9$, respectively, over $\alpha = 0.05$–0.95, $\beta = -0.2$ to 0.45 (see the right part of the α–β plane shown in Fig. 4). As demonstrated in the graphs, F_2 varies almost linearly with increasing α under fixed value of β. From the comparison between Figs. 10 and 11, it is seen that F_1 and F_2 vary in different ways depending on composite parameters α, β. It is found that the variations of F_1 and F_2 behave similarly as those shown in Fig. 10 when $a/W < 0.4$, and then they change the tendencies similarly as those shown in Fig. 11 when $a/W > 0.4$. The effect of the relative crack size will be depicted in Section 3.5.

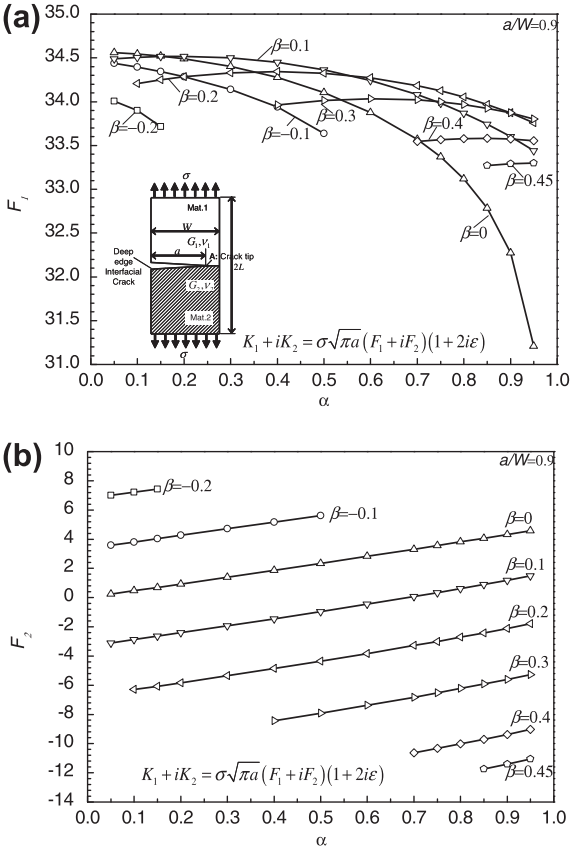

Fig. 11. Variations of: (a) F_1 and (b) F_2 with α, β for $a/W = 0.9$.

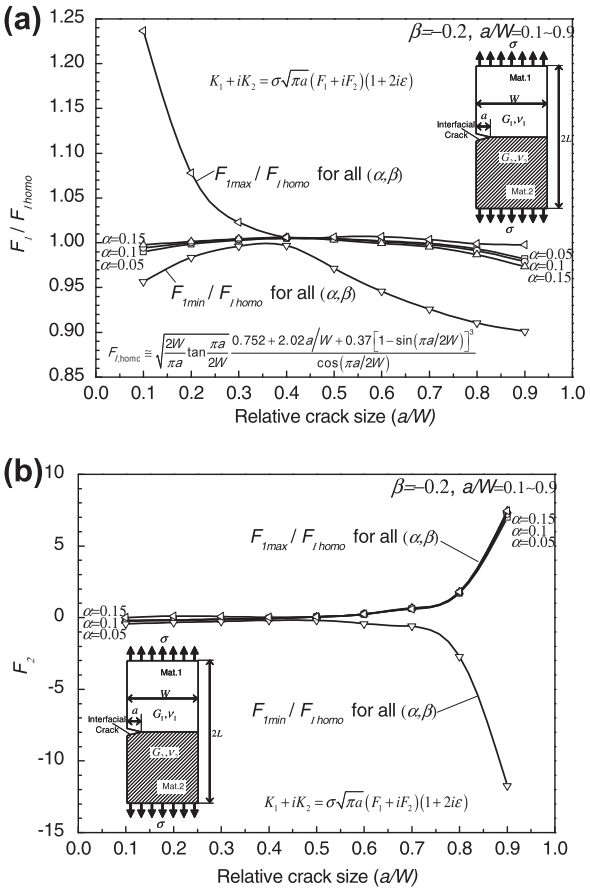

Fig. 12. Variations of: F_1 (a) and F_2 (b) with α, a/W for $\beta = -0.2$.

3.5. Effect of the relative crack size a/W on F_1, F_2

The variations of F_1, F_2 and their maximum and minimum values are plotted in Figs. 12–14 over $a/W = 0.1$–0.9 with varying material composite parameters. In order to examine the effect more clearly, the values of F_1 are normalized by using those of the homogenous plate. The values of the homogenous plate ($\alpha = \beta = 0$) $F_{I,\mathrm{homo}}$ are tabulated in Table 4. It is apparent from the table that the current results are in good agreement with the previous analytical solutions [21–23] with at least 4-digit accuracy. The values of $F_{I,\mathrm{homo}}$ can also be computed using Eq. (19) with an error within 0.59% [22].

$$F_{I,\mathrm{homo}} \cong \sqrt{\frac{2W}{\pi a}}\tan\frac{\pi a}{2W}\,\frac{0.752 + 2.02a/W + 0.37[1 - \sin(\pi a/2W)]^3}{\cos(\pi a/2W)} \tag{19}$$

Figs. 12a–14a clearly depict that there is an inflection point around $a/W = 0.4$ for arbitrary α, β regarding the tendency of $F_1/F_{I,\mathrm{homo}}$. Specifically, $F_1/F_{I,\mathrm{homo}}$ increases with increasing α under fixed β before this point, but increases with decreasing α after this point. However, F_2 increases monotonously with decreasing β for fixed α and a/W within the range of $0.1 < a/W < 0.9$, and increases monotonously with decreasing α for fixed β and a/W. In addition, over the whole range of α–β space, Fig. 13a shows that $F_1/F_{I,\mathrm{homo}}$ peaks at $\alpha = 0.95$, $\beta = 0$ when $a/W < 0.4$, but bottoms out at $\alpha = 0.95$, $\beta = 0$ when $a/W > 0.4$ for the whole α–β space. Fig. 14a shows $F_1/F_{I,\mathrm{homo}}$ reaches the lowest point at $\alpha = 0.85$, $\beta = 0.45$ when $a/W < 0.4$. However, the lowest point for $a/W > 0.4$ is not situated at one unique (α, β). From Figs. 12b–14b, it is found that F_2 peaks at $\alpha = 0.1$, $\beta = 0.2$ when $a/W < 0.4$ and at $\alpha = 0.15$, $\beta = -0.2$ when $a/W > 0.4$ for the whole α–β space. On the other hand, F_2 bottoms out at $\alpha = 0.95$, $\beta = 0$ when $a/W < 0.4$ and at $\alpha = 0.85$, $\beta = 0.45$ when $a/W > 0.4$. The exact maximum and minimum values of F_1, F_2 are listed in Table 5, and the corresponding material composite parameters α, β are also tabulated in the brackets.

4. Conclusions

In this paper, the finite element method focusing on the zero element at the crack tip was successfully applied into solving the stress intensity factors of the edge interface crack in a bi-material bonded dissimilar strip subjected to axis longitu-

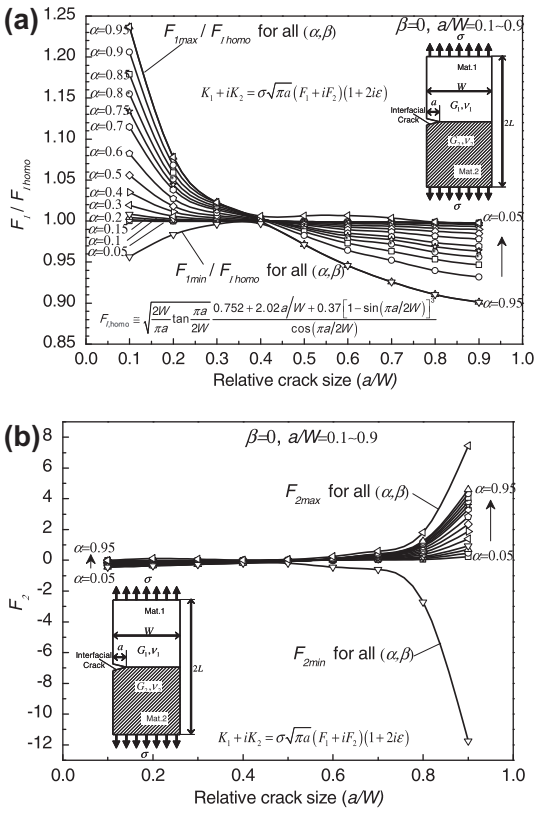

Fig. 13. Variations of: F_1 (a) and F_2 (b) with $\alpha, a/W$ for $\beta = 0$.

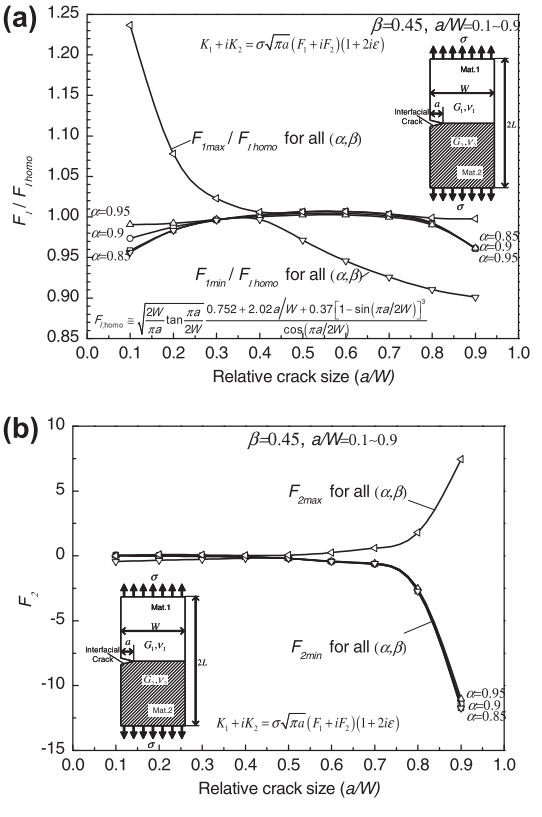

Fig. 14. Variations of: F_1 (a) and F_2 (b) with $\alpha, a/W$ for $\beta = 0.45$.

Table 4
The values of $F_{I,\mathrm{homo}}$ for the homogenous plate.

a/W	Kaya and Erdogan [21]	Noda et al. [22]	Current	Ref. [23]
→0	1.1215	1.1215	1.121	1.122
0.1	1.1892	1.189	1.189	1.196
0.2	1.3673	1.367	1.367	1.367
0.3	1.6599	1.659	1.660	1.655
0.4	2.1114	2.111	2.111	2.108
0.5	2.8246	2.823	2.824	2.827
0.6	4.0332	4.032	4.031	4.043
0.7	6.3549	6.355	6.352	6.376
0.8	11.955	11.95	11.95	11.99
0.9	34.633	34.62	34.60	34.72

Table 5
Maximum and minimum values of F_1 and F_2 for $0.1 < a/W < 0.9$.

a/W	$F_{1\min}(\alpha, \beta)$	$F_{1\max}(\alpha, \beta)$	$F_{2\min}(\alpha, \beta)$	$F_{2\max}(\alpha, \beta)$
0.1	1.138 (0.7, 0.4)	1.470 (0.95, 0)	−0.442 (0.95, 0.1)	−0.007 (0.05, 0.1)
0.2	1.345 (0.85, 0.45)	1.474 (0.95, 0)	−0.347 (0.95, 0)	0.108 (0.1, 0.2)
0.3	1.653 (0.85, 0.45))	1.698 (0.95, 0)	−0.270 (0.95, 0)	0.072 (0.1, 0.2)
0.4	2.105 (0.95, 0.3)	2.124 (0.15, −0.2)	−0.182 (0.95, 0)	0.020 (0.1, 0.2)
0.5	2.744 (0.95, 0)	2.843 (0.7, 0.4)	−0.195 (0.85, 0.45)	0.053 (0.05, −0.2)
0.6	3.814 (0.95, 0)	4.060 (0.85, 0.45)	−0.438 (0.85, 0.45)	0.243 (0.15, −0.2)
0.7	5.977 (0.95, 0)	6.378 (0.7, 0.4)	−1.011 (0.85, 0.45)	0.660 (0.15, −0.2)
0.8	10.885 (0.95, 0)	11.940 (0.15, 0.1)	−2.719 (0.85, 0.45)	1.810 (0.15, −0.2)
0.9	31.207 (0.95, 0)	34.559 (0.05, 0)	−11.741 (0.85, 0.45)	7.441 (0.15, −0.2)

dinal uniform tensile stress. The stress intensity factors were evaluated for the whole range of combinations of materials and the relative crack sizes. Then, variations of the dimensionless stress intensity factors F_1, F_2 for various relative crack size a/W were indicated for arbitrary material combinations and relative crack sizes. And the effect of material combination and relative crack size to the stress intensity factors were investigated systematically. Besides, since a linear relationship of $F_1, F_2 \propto (a/W)^{\lambda-1}$ was observed for the shallow edge crack case, a useful approximate function was proposed to compute the stress intensity factors for arbitrary material combinations.

References

[1] Williams ML. Stress singularities resulting from various boundary conditions in angular corners of plates in extension. J Appl Mech 1952;19:526–8.
[2] Bogy DB. Two edge-bonded elastic wedges of different materials and wedges angles under surface tractions. J Appl Mech 1971;38:377–86.
[3] Bogy DB, Wang KC. Stress singularities at interface corners in bonded dissimilar isotropic elastic materials. Int J Solids Struct 1971;7:993–1005.
[4] Hein VL, Erdogan F. Stress singularities in a two-material wedge. Int J Fract Mech 1971;7:317–30.
[5] Dempsey JP, Sinclair GB. On the stress singularities in the plane elasticity of the composite wedge. J Elast 1979;9:373–91.
[6] van Vroonhoven JCW. Stress singularities in bi-material wedges with adhesion and delamination. Fatigue Fract Engng Mater Struct 1992;15:157–71.
[7] Reedy ED, Guess TR. Composite to metal tubular lap joints: strength and fatigue resistance. Int J Fract 1993;63:351–67.
[8] Akisanya AR, Fleck NA. Interfacial cracking from the free edge of a long bimaterial strip. Int J Solids Struct 1997;34:1645–65.
[9] Xu JQ, Liu YH, Wang XG. Numerical methods for the determination of multiple stress singularities and related stress intensity coefficients. Engng Fract Mech 1999;63:775–90.
[10] Wu YL. A new method for evaluation of stress intensities for interface cracks. Engng Fract Mech 1994;48:755–61.
[11] Yang XX, Kuang ZB. Contour integral method for stress intensity factors of interface crack. Int J Fract 1996;78:299–313.
[12] Dong YX, Wang ZM, Wang B. On the computation of stress intensity factors for interfacial cracks using quarter point boundary elements. Engng Fract Mech 1997;57:335–42.
[13] Liu YH, Wu ZG, Liang YC, Liu XM. Numerical methods for determination of stress intensity factors of singular stress field. Engng Fract Mech 2008;75:4793–803.
[14] Oda K, Kamisugi K, Noda NA. Analysis of stress intensity factor for interface cracks based on proportional method. Trans JSME 2009;A75:476–82.
[15] Teranishi T, Nisitani H. Determination of highly accurate values of stress intensity factor in a plate of arbitrary form by FEM. Trans JSME 1999;A65:16–21.
[16] Noda NA, Zhang Y, Lan X, Takase Y, Oda K. Stress intensity factor of an interface crack in a bonded plate under uni-axial tension. J Solid Mech Mater Engng 4(7):974–87.
[17] Zhang Y, Noda NA, Takaishi KT, Lan X. Stress intensity factors of a central interface crack in a bonded finite plate and periodic interface cracks under arbitrary material combinations. Engng Fract Mech 2011;78:1218–32.
[18] Noda NA, Lan X, Michinaka K, Zhang Y. Stress intensity factor of an edge interface crack in a bonded semi-infinite plate. Trans JSME 2010;A76(770):1270–7 [in Japanese].
[19] Bogy DB. Edge-bonded dissimilar orthogonal elastic wedges under normal and shear loading. Trans ASME, J Appl Mech 1968;35:460–6.
[20] Chen DH, Nishitani H. Intensity of singular stress field near the interface edge point of a bonded strip. Trans JSME 1993;A59:2682–6.
[21] Kaya AC, Erdogan F. On the solution of integral equations with singular kernels. Quart Appl Math 1987;1(45):105–22.
[22] Noda NA, Araki K, Erdogan F. Stress intensity factors in two bonded elastic layers with a single edge crack under various loading conditions. Int J Fract 1992;A57:101–26.
[23] Tada H, Paris PC, Irwin GR. The stress analysis of cracks handbook. 3rd ed. New York: Maddm; 2000.